Photothermal Effects of Implanted Terahertz Biosensing Networks

Samar Elmaadawy and Josep Miquel Jornet
Institute for the Wireless Internet of Things
Department of Electrical and Computer Engineering
Northeastern University,
Boston, MA, USA
Email: {elmaadawy.s, j.jornet}@northeastern.edu

GLOBECOM 2024 - 2024 IEEE Global Communications Conference | 979-8-3503-5125-5/24/$31.00 ©2024 IEEE | DOI: 10.1109/GLOBECOM52923.2024.10901465

***Abstract*—Biosensors are shaping the future of healthcare through their vital role in disease detection, diagnostics, biomarker detection, and continuous health monitoring. In intra-body wireless nanosensor networks, biosensors are anticipated to incorporate antennas employing high frequencies, including the terahertz frequency band. Terahertz technology facilitates fast communication and the creation of compact designs. However, photothermal effects will be induced due to the absorption of the radiation by the tissue. In this paper, a photothermal model is developed on COMSOL Multiphysics® to explore the impact of the implanted biosensor electromagnetic radiation on the skin. According to the model's findings, the increase in the skin's temperature is proportional to the increase in both the transmission power and the number of biosensors in the network. Furthermore, power fluctuations resulting from the presence of multiple biosensors are found to be separate and distinct from temperature variations in the tissue. This indicates that at certain points in the skin, the power level might be moderate, but the temperature is high. Such analysis is beneficial to better understand the photothermal effects of the terahertz radiation from implanted devices and to define safe deployment guidelines.**

***Index Terms*—Biosensor, healthcare, terahertz (THz), photothermal, implanted devices, deployment guidelines**

I. Introduction

Biosensing utilizes miniature devices to identify and detect biomolecules, revealing details about their activity and concentration within a biological environment. This technology holds immense potential in healthcare, offering advancements in biomonitoring, disease diagnosis, and even treatment. Miniature biosensors can be worn around the body or implanted either in a fixed location, such as the skin layer or on an organ, or flowing, for example, in the bloodstream or through the digestive tract. The field of biosensors is currently experiencing a thrilling transformation as nanoantennas are being incorporated, facilitating remote communication with a neighboring biosensor or a central receiver (such as a wearable or a scanning device). These biosensors, also called biomachines, combine the biorecognition capabilities of conventional biosensors with the efficiency of wireless data transmission, enabling real-time and remote health monitoring [1]. Biorecognition is based on an element (i.e., enzyme, antibody, or nucleic acid) that interacts with a target analyte in the body, measuring the biological response and converting it into an electrical signal. The incorporated antenna transmits the signal through body cells/tissues to be detected by the wearable receiver. Potential applications for this technology are wide-ranging, including, but not limited to, continuous glucose monitoring [2], detecting infectious diseases [3], and even cancer monitoring [4]. For example, glucose biosensors could be implanted in a diabetic patient to wirelessly transmit information to a wearable receiver offering continuous blood sugar monitoring.

Among the different technologies to interconnect nanosensors, including molecular [5], acoustic [6], and coupling-based [7] communication techniques, electromagnetic communications at terahertz frequencies are being considered because of their unique properties that will benefit this industry in many ways. High frequency translates to short wavelength, which enables the production of compact antennas and devices. In contrast to lower frequencies, terahertz technology offers micro- or even nanoscale designs, paving the way for the implanted and wearable biosensors era [8]. Additionally, using graphene in plasmonic-based antennas could result in more compact designs [9]. To illustrate, a biosensor circulating in the blood has to be significantly minuscule to easily flow through the bloodstream and to prevent the risk of clogging. Terahertz radiation can also be focused into a high-gain narrow beam for ideal selectivity, facilitating precise targeted analysis while limiting interference from other particles in the medium [10]. Focusing the beam in the intentional direction is energy efficient, as it minimizes energy waste in undesired directions. However, for the device to have directional capabilities, its size needs to be slightly enlarged. This flexibility allows for optimization based on the intended use case.

In addition to that, terahertz technology provides high bandwidth communication and high data rates, reaching terabits per second. The requirement for fast communication may not always be critical in intra-body network applications. However, this fast communication may reduce the time the human skin is exposed to radiation. Besides communication, terahertz waves are sensitive to changes in the dielectric properties of biological tissues and cells. This helps in understanding biological processes and detecting potential diseases [11].

In the last decade, many research efforts worldwide have been aimed at developing new transceivers and antennas

This work was funded by NSF grant CBET-2039189.

Authorized licensed use limited to: Northeastern University. Downloaded on June 09,2025 at 20:35:32 UTC from IEEE Xplore. Restrictions apply.

for implantable biosensors [9], studying the propagation of terahertz signals within the human body [12], and designing communication and networking protocols to provide reliable connectivity to intra-body devices [13]. Despite being considered a promising candidate for biosensor communication in intra-body networks, the potential photothermal effects of terahertz implanted or wearable devices remain obscure.

Essentially, the thermal dynamics of single and multiple implants have been previously studied, for example, in [14]. In this work, the biosensors are not wirelessly connected; thus, the device's operational power is the main cause of the temperature change in the tissue. For wireless bioimplants, in addition to the heat generated by the device, the absorption of electromagnetic radiation contributes to the overall temperature change in the tissue. This problem was addressed before at low frequencies (in MHz) in [15], and only recently have the photothermal effects of terahertz radiators been explored. Advantageously, terahertz electromagnetic radiation is non-ionizing (i.e., it does not break molecular bonds); hence, it does not change the structure of the molecule, making it safe for biological applications. However, as the tissue's absorption coefficient is higher at terahertz frequencies than at lower frequencies, the skin, tissue, and cells will absorb more radiation, which will then be transferred into thermal energy, contributing to the overall temperature rise. Early models of outside-the-body penetration of THz signals and photothermal effects were introduced and studied in [16], [17]. For within-the-body radiation, [18] relied on simplifying closed-form equations to evaluate the photothermal effect of terahertz radiation but did not consider the combination of the skin layers and blood vessels in the model; rather, it examined each independently without accounting for the role of blood in regulating the skin temperature. Additionally, [19] focuses on a single transmitter in a group of red blood cells, which may not fully capture the complexity of interactions in real scenarios.

In this paper, we present the photothermal effect of blood-flowing and tissue-implanted biosensors operating at true terahertz frequencies. More specifically, we develop a multi-physics model that combines modeling the wave propagation in the skin and evaluating the generated heat due to absorbing the radiation, considering the blood perfusion factor for regulating the skin temperature. We then utilize this model to study the thermal impact of implanted nanonetworks in two different scenarios commonly found in the related literature, namely, within the blood vessels and across tissues to the wearable device. For all these, we utilize realistic values of critical system parameters, including biosensor transmit power and radiation diagrams and the electromagnetic properties of body tissues at terahertz frequencies. The results show that terahertz radiation absorption induces heat within human skin. However, this effect can be controlled through the implementation of low-power transmission biosensors, along with careful consideration of the spacing between implanted biosensors.

The remainder of the paper is organized as follows: We describe the system model, which is composed of human skin and implanted devices, in Sec. II. Then, in Sec. III, the developed multiphysics model is introduced, and all considered scenarios are presented. Finally, we analyze and discuss the results in Sec. IV with the conclusions and future work highlighted in Sec. V.

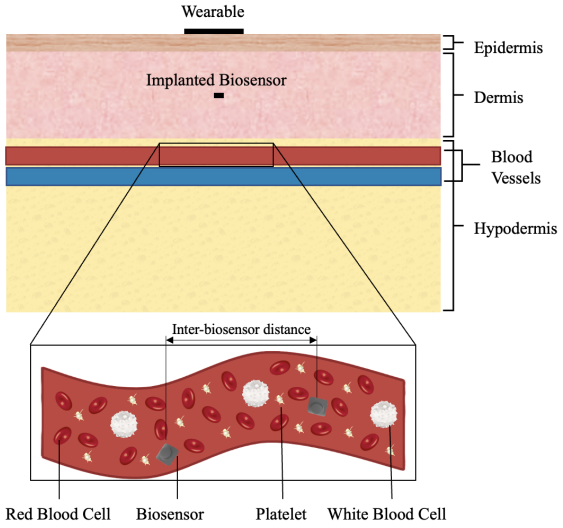

Fig. 1: The developed model in COMSOL®.

II. System Model

The system framework of this study is formed of the skin layers and implanted biosensors.

A. Skin Layers

Human skin is the largest body organ that acts as a protective barrier from external factors such as heat, bacteria, and infections. The skin comprises 3 layers that vary in thickness and texture all over the body depending on gender, age, health conditions, and fitness [20].

Epidermis is the thin outer layer of the human body that is made of mostly keratinocyte cells. This layer is the principal protector of the skin, prevents water loss, produces new skin cells, and determines skin color. Its thickness varies between 0.04 mm at the eyelid and 0.16 mm at the palms and soles. The wearable device is attached to this layer. **Dermis** is the middle skin's strong base layer that is made up of collagen and elastin fiber-rich connective tissue. The skin's strength and suppleness are derived from these protein fibers, enabling the skin to move and bend without breaking. Moreover, the dermis contains sweat glands, nerves, hair follicles, and very thin blood vessels. The thickness of this layer varies between 1 mm and 2.8 mm. A biosensor is implanted in this layer, acting as a hub to ensure signal reception at the wearable device. **Hypodermis**, often called the subcutaneous adipose tissue layer, offers temperature regulation and energy storage. This layer comprises loose connective tissue, adipocytes (i.e., fat cells), and blood vessels, where biosensors are flowing. The underlying muscles and bones are also mechanically cushioned and padded by the hypodermis, protecting them from impact

Authorized licensed use limited to: Northeastern University. Downloaded on June 09,2025 at 20:35:32 UTC from IEEE Xplore. Restrictions apply.

and pressure from the outside world. Its thickness varies between less than 1 mm in the eyelid and 3 cm in the abdomen.

B. Biosensors Deployment

As previously mentioned, biosensors can either flow within the bloodstream or be implanted in a specific location within the skin. In certain applications, only flowing biosensors are utilized, capable of communicating directly with the wearable device. However, other applications may necessitate the use of an additional hub, usually at the dermis layer, to facilitate communication with the wearable sensor. Accordingly, we examine both scenarios: communication among biosensors within the bloodstream and communication across skin layers, as shown in Fig. 1.

III. Analytical Methodology

A. Multiphysics Modeling

This section details a photothermal 2D model built on COMSOL Multiphysics® Simulation Software, which is based on the Finite Element Method (FEM) analysis. This model aims to study the photothermal effects of terahertz radiation emitted from implanted biosensors to communicate with an outside wearable device. The model geometry comprises three skin layers: epidermis, where the wearable biosensors are attached; dermis; and hypodermis, where the implanted biosensors are confined inside the blood vessels, as illustrated in Fig. 1.

Following a similar methodology as in [21], the model starts with first computing the power density distribution in the different domains and then evaluates the heat generated in the medium exposed to electromagnetic radiation. More specifically, we use the diffusion approximation of the Radiative Transfer Equation (RTE) to describe the power intensity distribution within the medium. This approximation assumes isotropic scattering and ignores higher-order scattering events. In our case, the scattering coefficient is negligible since in terahertz intrabody propagation, the main loss factor is the absorption coefficient [22]. The approximated equation used to develop this part of the model is as follows:

$$\left(\frac{1}{v}\frac{\partial}{\partial t} - D\nabla^2 + \mu_a\right)\Phi(\overrightarrow{r},t) = q_0(\overrightarrow{r},t), \tag{1}$$

where v is the speed of light, $D = \frac{1}{3}\mu_a$ is the diffusion coefficient, μ_a is the absorption coefficient, $\Phi(\overrightarrow{r},t)$ is the fluence rate, and $q_0(\overrightarrow{r},t)$ is the source.

Then, we use Pennes' Bioheat Equation (PBE) to describe the heat transfer within the biological medium. The model uses the power density distribution data from the previous step and estimates the temperature distribution in the medium according to the following equation:

$$\rho C_p \frac{\partial T}{\partial t} = k\nabla^2 T - w_b\rho_b C_{p_b}(T_a - T) + Q_{met} + Q_{rad}, \tag{2}$$

where ρ is the medium density, C_p is the specific heat capacity, T is the temperature, k is the thermal conductivity, w_b is the blood perfusion rate, ρ_b is the blood density, C_{p_b} is the blood specific heat capacity, T_a is the arterial blood temperature, Q_{met} is the metabolic heat generation rate per unit volume of tissue, and Q_{rad} is the radiation heat source.

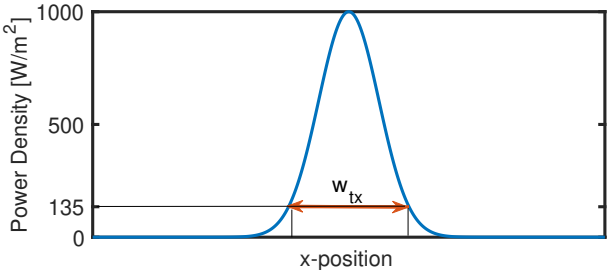

Fig. 2: Gaussian Beam.

All the electrical and thermal parameters in the previous equations are required for each defined medium in the model. The electrical parameters for frequency = 1 THz, found in [23]–[26], and the thermal parameters, found in [20], [27], [28], are presented in Table I. Furthermore, within the dermis and hypodermis layers, the blood perfusion rate is 0.00125 1/s, whereas in the epidermis, it is absent owing to the lack of blood circulation within this particular layer. Blood comprises about 55% plasma, 45% Red Blood Cells (RBC), and less than 1% of white blood cells and platelets [29]. Therefore, to reduce the model complexity, only plasma and RBC are considered.

TABLE I: Model parameters for frequency = 1 THz.

Parameter	Unit	Epidermis	Dermis	Hypodermis	Plasma	RBC
n	-	1.8	2.1	1.55	2.15	2.13
μ_a	$1/cm$	70	20	22	225	180
ρ	kg/m^3	1200	1200	1000	1020	1093
k	$W/(m.K)$	0.24	0.45	0.19	0.58	0.46
C_p	$J/(kg.K)$	3590	3330	2500	3930	3210
Thickness	mm	0.1	1	2	0.2	0.008

The radiation source in the model is defined as a Gaussian beam with a parametric maximum power density value that can be modified based on each scenario. The beam's power density profile is given by:

$$P_d = P_{d_{max}} e^{-2(\frac{x}{w_{tx}})^2}, \tag{3}$$

and the power, in dBm, at each point in the model is calculated according to the following equation:

$$P = 10\log_{10}\left(\frac{P_d}{\text{Mesh element area}}\right) + 30, \tag{4}$$

where P_d is the power density, x manifests the beam location, w_{tx} is the width of the beam where the maximum power density drops to $1/e^2$, (i.e., around 13.5%) of the maximum value, as shown in Fig. 2, and P is the power in dBm.

B. Methodological Planning and Considerations

Utilizing this model, a comprehensive analysis is conducted across various scenarios. Initially, the photothermal effects of

Authorized licensed use limited to: Northeastern University. Downloaded on June 09,2025 at 20:35:32 UTC from IEEE Xplore. Restrictions apply.

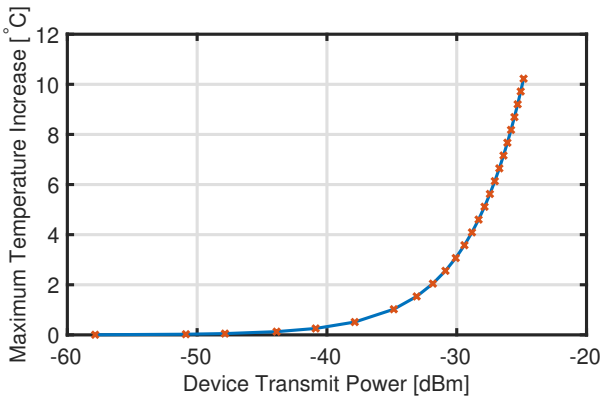

Fig. 3: The maximum temperature increase caused by the radiation of a single implanted device operating at 1 THz in the blood, as a function of the transmitted power.

the radiation from a single biosensor flowing in the blood at different power levels are investigated to understand terahertz propagation and study the effect of the transmitting power on the tissue temperature. This investigation enables the establishment of a maximum permissible transmit power limit to prevent overheating of the skin. Subsequently, the effect of the distance between flowing biosensors is examined. Whether the biosensors need to communicate or not, the inter-biosensor distance must be carefully selected for each application based on the required power while maintaining body temperature. Finally, the photothermal effect of terahertz radiation from one dermal layer implant and several blood-flowing biosensors is demonstrated, illustrating variations in power levels and temperature within the blood vessel.

From now on, the operating frequency of all the presented transmitters is 1 THz. It is also assumed that the biosensor antenna size equals the width of the Gaussian beam. The term "power density" refers to the maximum power density specified for the biosensor. Finally, the biosensor location is marked in purple in each figure.

IV. Results and Discussions

A. Single Implant in Blood

Our analysis starts first by focusing on a single blood-implanted biosensor. This device is intended to communicate with a wearable, a stationary implanted device, or a nearby biosensor that is also flowing through the bloodstream. Fig. 3 depicts the thermal impact of the device's electromagnetic radiation across various power levels. The maximum temperature increase within the tissue grew exponentially with increasing the device's transmit power, even after taking into account the effect of blood perfusion, which regulates tissue temperature. In order to guarantee that the tissue does not experience excessive heat, a transmission power limit of -38 dBm, or approximately 1 mW/mm^2, is set. This restriction ensures that the radiation from a single device will prevent raising the tissue temperature by more than $1°C$.

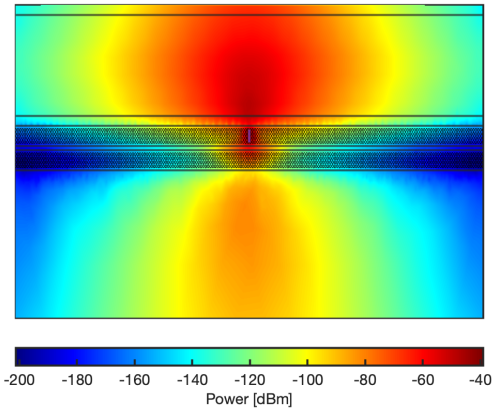

(a)

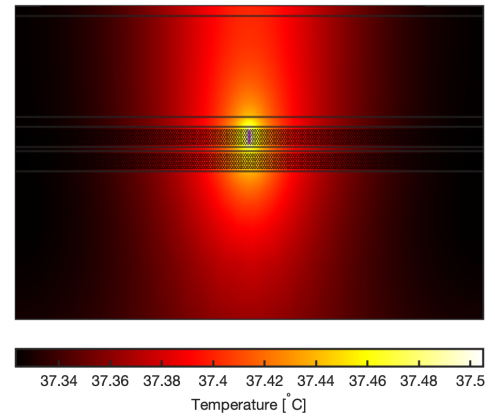

(b)

Fig. 4: (a) The electromagnetic wave propagation, and (b) the temperature change in the tissue due to a single 1 THz implanted device with transmit power = -38 dBm in the blood vessel.

The power generated by a single device is presented in Fig 4a. This is the highest power that can be used in the current scenario without causing tissue burns or cell death. Due to the high absorption coefficients of red blood cells and plasma, a significant amount of power was lost/absorbed before leaving the blood vessel, making the total power loss near the epidermal surface around 27 dB. In some applications and designs, this power loss could be acceptable; however, in other cases, more power is required for the wearable sensor to detect the signal. As a result of the absorption of the radiation for 10 minutes, electromagnetic energy was transformed into thermal energy, causing the device to act as a heat source within the blood vessel, as illustrated in Fig. 4b.

B. Separation of Biosensors in the Blood

For precise diagnosis and treatment, multiple biosensors are expected to be flowing in the blood vessel. Increasing the number of implanted devices will increase the power received by the wearable sensor, raising the overall tissue's

Authorized licensed use limited to: Northeastern University. Downloaded on June 09,2025 at 20:35:32 UTC from IEEE Xplore. Restrictions apply.

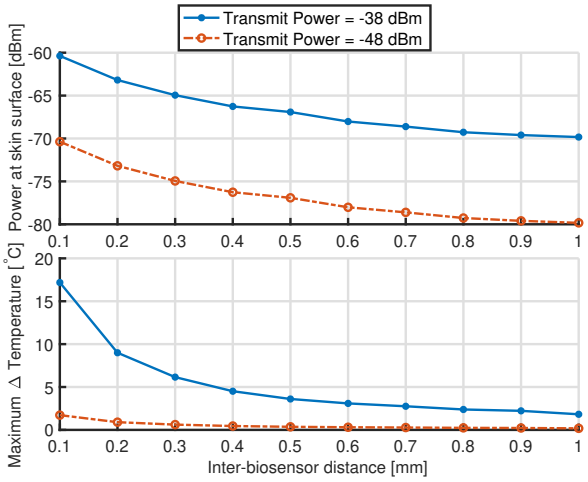

Fig. 5: The variation in the received power at the epidermis layer and the maximum temperature change in the skin due to changing the distance between biosensors.

temperature. In this regard, we shall transmit less power from each implanted device and regulate the distance between the biosensors. Therefore, Fig. 5 presents the effect of inter-biosensor distance on the power received at the epidermis surface and the overall tissue temperature after 10 minutes of exposure to the radiation. Two different transmit powers were considered: -38 dBm and -48 dBm. Previously, the maximum permissible power to be emitted from a single biosensor was set to -38 dBm. However, when the number of biomachines increases, the overall received power at a point increases, increasing the skin's temperature. The figure depicts that both the power received at the epidermal surface as well as the maximum increase in skin temperature decrease with increasing the distance between incorporated biomachines in the blood. When the transmit power changed from -38 dBm to -48 dBm, a 10 dB power difference was recognized at the epidermal surface. However, the temperature of the skin was significantly affected, especially at low inter-biosensor distances. Moreover, the bigger the inter-biosensor distance, the harder it is for the biomachines to communicate. Therefore, it is advantageous to have biosensors close to one another emitting lower power to facilitate communication between biomachines while maintaining the temperature of the human skin.

C. Biosensors Across the Blood and Skin Layers

Given that increasing the transmission power from a single biosensor causes a remarkable increase in the skin's temperature, an additional hub/repeater, which is an extra implanted device, might sometimes be required in the dermis layer. Consequently, a scenario in which the implanted standing biosensor in the dermis layer is considered along with the blood-flowing biosensors, with each device transmitting a power of around -48 dBm and a blood inter-biosensor distance of 0.4 mm. The power distribution over the modeled skin surface is shown in Fig. 6a. It is noteworthy to observe that only a very small amount of radiation was capable of penetrating deeply into the body. This figure also clearly illustrates that the radiation is significantly absorbed in the blood vessels compared to the dermal tissue. As a result of the radiation, the change in the skin temperature is the highest around high-power areas, as presented in Fig. 6b. It can be highlighted that the propagation of electromagnetic energy in the body differs from that of thermal energy. Accordingly, the corresponding temperature and power level fluctuations along the blood vessel (i.e., along the line between the black arrows, where flowing biosensors are implanted) are depicted in Fig. 6c. Each power peak shows where one implant is located. The temperature continued to rise until it reached the center of the modeled blood vessel, at which the dermis layer biosensor thermal impact was greatest. The minor peaks in the curve represent the photothermal impact of each biosensor radiation, and the main peak in the temperature graph represents the photothermal impact of the dermal tissue implant radiation. This is merely the result of the temperature rise compounded by the electromagnetic radiation from the standing dermal biosensor and all of the blood biosensors.

V. Conclusions and Future Work

This paper has provided an in-depth investigation into the thermal effects of implanted terahertz biosensors in intra-body wireless nanosensor networks, as well as defining some requirements for effective communication in the network. Terahertz radiation from biomachines introduces thermal effects in the human body, but it can be regulated to ensure safe deployment. Both the power transmitted from the device and the number of incorporated biosensors in the network influence the overall temperature increase in the surrounding tissue. Hence, as the number of implanted biosensors increases, the power emitted by each sensor should decrease to prevent overheating the medium, which can then cause cell death and tissue damage. Given that blood absorbs electromagnetic radiation significantly, implanted devices in the blood must be close to each other to be detectable. Also, an implanted biosensor in the dermis layer beneath the wearable device might be required to ensure that the signal transmitted from the blood biosensors arrives at the wearable. Ultimately, the fluctuations of the tissue temperature are distinct from those for electromagnetic propagation. As a prospect for future research, it is worth noting that this developed model accommodates transients and temporal variations. All presented findings are based on 10 minutes of exposure to terahertz radiation. However, given the fast data rates that terahertz technology provides, continuous device operation may not be necessary, enabling the transmission of pulses instead. This aspect requires further investigation.

References

[1] D. Rodrigues, A. I. Barbosa, R. Rebelo, I. K. Kwon, R. L. Reis, and V. M. Correlo, "Skin-integrated wearable systems and implantable biosensors: a comprehensive review," *Biosensors*, vol. 10, no. 7, p. 79, 2020.

Authorized licensed use limited to: Northeastern University. Downloaded on June 09,2025 at 20:35:32 UTC from IEEE Xplore. Restrictions apply.

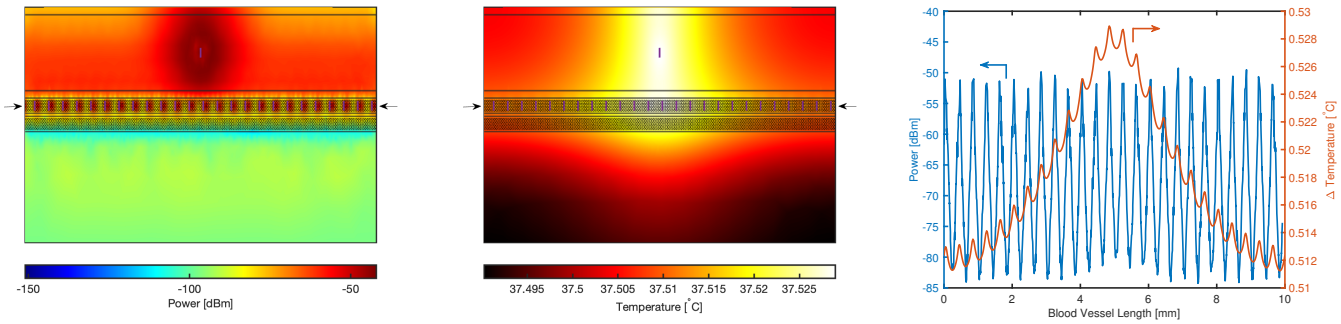

(a) (b) (c)

Fig. 6: (a) Power distribution, (b) temperature profile of the modeled skin, and (c) the changes in power and temperature along the blood vessel.

[2] S. Kim, J. Malik, J. M. Seo, Y. M. Cho, and F. Bien, "Subcutaneously implantable electromagnetic biosensor system for continuous glucose monitoring," *Scientific Reports*, vol. 12, no. 1, p. 17395, 2022.

[3] K. E. Mach, P. K. Wong, and J. C. Liao, "Biosensor diagnosis of urinary tract infections: a path to better treatment?," *Trends in pharmacological sciences*, vol. 32, no. 6, pp. 330–336, 2011.

[4] J. Jornet, L. Feng, E. P. Furlani, Q. Gan, Z. Sun, and Y. Wu, "Smart healthcare system," Aug. 9 2022. US Patent 11,406,266.

[5] M. M. Al-Zubi, A. S. Mohan, P. Plapper, and S. H. Ling, "Intrabody molecular communication via blood-tissue barrier for internet of bio-nano things," *IEEE Internet of Things Journal*, vol. 9, no. 21, pp. 21802–21810, 2022.

[6] F. Dressler and S. Fischer, "Connecting in-body nano communication with body area networks: Challenges and opportunities of the internet of nano things," *Nano Communication Networks*, vol. 6, no. 2, pp. 29–38, 2015.

[7] A. Vizziello, M. Magarini, P. Savazzi, and L. Galluccio, "Intra-body communications for nervous system applications: Current technologies and future directions," *Computer Networks*, vol. 227, p. 109718, 2023.

[8] J. M. Jornet and I. F. Akyildiz, "Graphene-based plasmonic nano-antenna for terahertz band communication in nanonetworks," *IEEE Journal on selected areas in communications*, vol. 31, no. 12, pp. 685–694, 2013.

[9] A. Sangwan and J. M. Jornet, "Beamforming optical antenna arrays for nano-bio sensing and actuation applications," *Nano Communication Networks*, vol. 29, p. 100363, 2021.

[10] A.-A. A. Boulogeorgos, J. M. Jornet, and A. Alexiou, "Directional terahertz communication systems for 6G: Fact check," *IEEE Vehicular Technology Magazine*, vol. 16, no. 4, pp. 68–77, 2021.

[11] O. Smolyanskaya, N. Chernomyrdin, A. Konovko, K. Zaytsev, I. Ozheredov, O. Cherkasova, M. Nazarov, J.-P. Guillet, S. Kozlov, Y. V. Kistenev, *et al.*, "Terahertz biophotonics as a tool for studies of dielectric and spectral properties of biological tissues and liquids," *Progress in Quantum Electronics*, vol. 62, pp. 1–77, 2018.

[12] W. Aman, M. M. U. Rahman, H. T. Abbas, M. A. Khalid, M. A. Imran, A. Alomainy, and Q. H. Abbasi, "Securing the insecure: A first-line-of-defense for body-centric nanoscale communication systems operating in THz band," *Sensors*, vol. 21, no. 10, p. 3534, 2021.

[13] A.-J. Garcia-Sanchez, R. Asorey-Cacheda, J. Garcia-Haro, and J.-L. Gomez-Tornero, "Dynamic multihop routing in terahertz flow-guided nanosensor networks: A reinforcement learning approach," *IEEE Sensors Journal*, vol. 23, no. 4, pp. 3408–3422, 2023.

[14] S. Kim, P. Tathireddy, R. A. Normann, and F. Solzbacher, "Thermal impact of an active 3-D microelectrode array implanted in the brain," *IEEE Transactions on Neural Systems and Rehabilitation Engineering*, vol. 15, no. 4, pp. 493–501, 2007.

[15] G. Lazzi, "Thermal effects of bioimplants," *IEEE Engineering in Medicine and Biology Magazine*, vol. 24, no. 5, pp. 75–81, 2005.

[16] I. V. K. Reddy, S. Elmaadawy, E. P. Furlani, and J. M. Jornet, "Multi-physics analysis of electromagnetic wave propagation and photothermal heating in human tissues at terahertz and optical frequencies," *Scientific Reports*, 2023.

[17] S. Elmaadawy and J. M. Jornet, "The thermal impact of wireless sub-terahertz radios on the human eye in next-generation extended reality headsets," *IEEE Future Networks World Forum*, 2023. In Press.

[18] H. Elayan, R. M. Shubair, and J. M. Jornet, "Characterising THz propagation and intrabody thermal absorption in iWNSNs," *IET Microwaves, Antennas & Propagation*, vol. 12, no. 4, pp. 525–532, 2018.

[19] H. Elayan, P. Johari, R. M. Shubair, and J. M. Jornet, "Photothermal modeling and analysis of intrabody terahertz nanoscale communication," *IEEE Transactions on Nanobioscience*, vol. 16, no. 8, pp. 755–763, 2017.

[20] M. Fu, W. Weng, and H. Yuan, "Numerical simulation of the effects of blood perfusion, water diffusion, and vaporization on the skin temperature and burn injuries," *Numerical Heat Transfer, Part A: Applications*, vol. 65, no. 12, pp. 1187–1203, 2014.

[21] I. V. K. Reddy and J. M. Jornet, "Multi-physics analysis of electromagnetic wave propagation and photothermal heating in human tissues at terahertz and optical frequencies," in *2022 18th International Conference on Distributed Computing in Sensor Systems (DCOSS)*, pp. 357–363, IEEE, 2022.

[22] H. Elayan, R. M. Shubair, J. M. Jornet, and P. Johari, "Terahertz channel model and link budget analysis for intrabody nanoscale communication," *IEEE transactions on nanobioscience*, vol. 16, no. 6, pp. 491–503, 2017.

[23] O. P. Cherkasova, D. S. Serdyukov, E. F. Nemova, A. S. Ratushnyak, A. S. Kucheryavenko, I. N. Dolganova, G. Xu, M. Skorobogatiy, I. V. Reshetov, P. S. Timashev, *et al.*, "Cellular effects of terahertz waves," *Journal of Biomedical Optics*, vol. 26, no. 9, pp. 090902–090902, 2021.

[24] N. Chopra, K. Yang, Q. H. Abbasi, K. A. Qaraqe, M. Philpott, and A. Alomainy, "THz time-domain spectroscopy of human skin tissue for in-body nanonetworks," *IEEE Transactions on Terahertz Science and Technology*, vol. 6, no. 6, pp. 803–809, 2016.

[25] E. Pickwell and V. Wallace, "Biomedical applications of terahertz technology," *Journal of Physics D: Applied Physics*, vol. 39, no. 17, p. R301, 2006.

[26] K. Jeong, Y.-M. Huh, S.-H. Kim, Y. Park, J.-H. Son, S. J. Oh, and J.-S. Suh, "Characterization of blood using terahertz waves," *Journal of biomedical optics*, vol. 18, no. 10, pp. 107008–107008, 2013.

[27] V. M. Nahirnyak, S. W. Yoon, and C. K. Holland, "Acousto-mechanical and thermal properties of clotted blood," *The Journal of the Acoustical Society of America*, vol. 119, no. 6, pp. 3766–3772, 2006.

[28] P. A. Hasgall, F. Di Gennaro, C. Baumgartner, E. Neufeld, B. Lloyd, M.-C. Gosselin, D. Payne, A. Klingenböck, and N. Kuster, "IT'IS Database for thermal and electromagnetic parameters of biological tissues." Version 4.1, Feb. 2022. DOI: 10.13099/VIP21000-04-1, https://itis.swiss/database.

[29] K. S. Saladin, *Human anatomy*. Rex Bookstore, Inc., 2005.

Authorized licensed use limited to: Northeastern University. Downloaded on June 09,2025 at 20:35:32 UTC from IEEE Xplore. Restrictions apply.